Using least-squares Kirchhoff migration for better shallow imaging of spatially sparse dual-WAZ data

Huifeng Zhu, Mustafa Al-Waily, Zheng Chang, and Zhuocheng Yang (CGG)*

Summary

Compared to narrow azimuth (NAZ) surveys, wide azimuth (WAZ) surveys are favored in the deepwater Gulf of Mexico (GOM) due to their large crossline offsets, which offer good subsurface illumination. Preprocessing technologies like 3D deghosting can recover the high temporal frequency content from WAZ; however, WAZ's sparse spatial sampling, e.g., 60 m inline bin size, tends to limit our ability to push for high resolution when imaging shallow targets near the water bottom. In the deepwater GOM, there is typically more than one WAZ survey available in different azimuths, which can potentially improve trace density. However, direct Kirchhoff imaging of each of the multiple data sets suffers from poor swing cancellation, especially in directions orthogonal to each WAZ acquisition direction. To mitigate this problem, we can combine multi-WAZ data and perform interpolation prior to Kirchhoff migration. Interpolation provides a uniform spatial sampling to reduce migration swings but is often challenging for complex structures and smears details. We propose an alternative approach using preconditioned least-squares (LS) Kirchhoff migration to obtain a higher resolution image that can simultaneously benefit from the recorded dual-WAZ data sets and overcome the limitation of coarse surface sampling.

Introduction

With multiple sources and more than one streamer vessel, wide azimuth (WAZ) surveys provide a larger offset-azimuth footprint over narrow azimuth (NAZ) surveys to help subsalt imaging (typically at lower frequencies). On the other hand, exploiting the high frequency information recorded in WAZ data sets for shallow imaging is very challenging due to the sparse spatial sampling, e.g., 60 m inline spacing. If multiple WAZ surveys are available, as is the case in most areas of the deepwater Gulf of Mexico (GOM), the trace coverage can be improved, especially in the case of surveys acquired orthogonal to each other. We can co-bin multiple WAZ surveys with smaller bin size and use pre-migration interpolation to fill in the empty bins and merge multiple WAZ surveys together. However, significant azimuthal differences in the input data limit the effectiveness of pre-migration interpolation. Therefore, we are faced with the challenge of how to fully exploit the benefits of multiple WAZ surveys for high fidelity shallow imaging.

Least-squares (LS) migrations (Shuster, 1993) based on migration and demigration operators have been developed to account for uneven acquisition geometry, complex overburdens, and migration artifacts. Wang et al. (2016) proposed an inverse Hessian approximation for the first iteration of LS migration. Later, Wang et al. (2017) extended that approach to multiple iterations of LS migration with preconditioned gradients.

Here, we use the preconditioned LS migration approach outlined by Wang et al. (2017) to migrate the dual-WAZ data together, obtaining a high-resolution shallow Kirchhoff image with improved S/N. The proposed flow performs the dual-WAZ data migration from their original trace positions without interpolation, which is essential to retain the recorded high frequency information.

Dual-WAZ data

Our study area is situated in Alaminos Canyon in the GOM. There are two surveys in this area: Survey 1 is a WAZ survey with an acquisition design modified to obtain large offsets up to 14 km, and Survey 2 is a conventional WAZ acquisition survey with 8.3 km maximum offset. Survey 1 was acquired in an east-west direction (Figure 1) with a 10 m shot depth and a slant-towed receiver profile ranging from 10 m (near channel) to 30 m (far channel). Survey 2 was acquired in a northeast-southwest direction (Figure 1) with a 10 m shot depth and constant 15 m receiver depth. The receiver and cable spacing are 12.5 m and 120 m, respectively, for both surveys. For this study, we focused on the shallow complex overburden, so we limited our analysis to (near) offsets up to 2100 m.

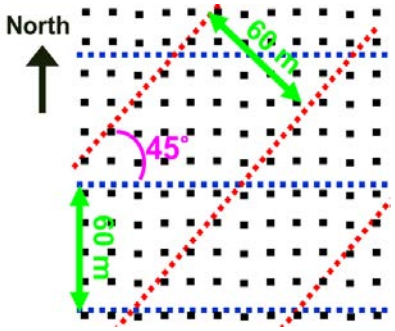

Figure 1: Blue dots represent traces from Survey 1 and red dots represent traces from Survey 2. On a 12.5 m x 12.5 m subsurface grid, as represented by black dots, traces from Survey 1 and Survey 2 are very sparse.

Since the two surveys were acquired at different times and with different objectives, they are markedly different in

10.1190/segam2018-2995491.1

their spectral content. To improve the data similarity between the two surveys, some key pre-processing steps were required. The data pre-processing included the following steps: noise attenuation, receiver motion correction, water column statics and tide corrections, 3D source-receiver deghosting (Wang et al., 2014), designature, and survey matching. Water column statics and tide corrections handled the water velocity and tidal status differences between the two surveys. 3D deghosting reduced frequency spectrum inconsistency by removing different receiver ghost notches due to different towing depths and re-datumed the data to the same sea level datum. Gun signature difference was removed by designature, followed by a matching filter to further match Survey 2 to Survey 1. The processed data sets were then used as the input to Kirchhoff migrations.

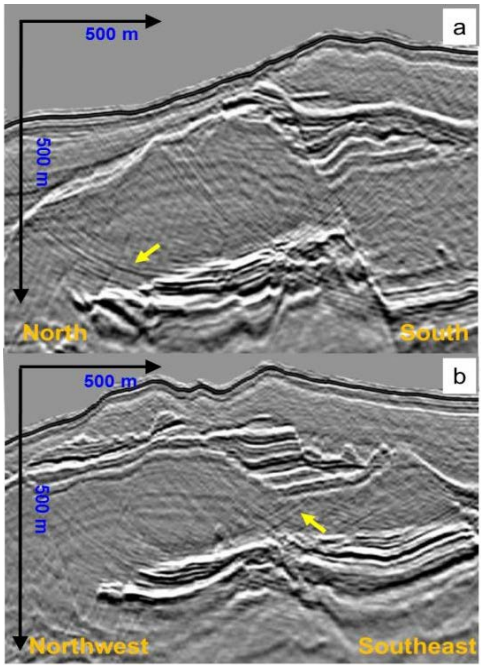

Figure 2: Images from dual-WAZ Kirchhoff migration without interpolation are displayed. In the (a) north-south and (b) northwest-southeast directions, orthogonal to Survey 1 and Survey 2's acquisitions respectively, severe migration swings (yellow arrows) are observed.

Poor migration swing cancellation

The dual-WAZ data sets were recorded on a 6.25 m x 60 m subsurface grid per their receiver and cable spacing configuration. The two data sets were binned together and then jointly migrated using Kirchhoff migration. For shallow imaging purposes, the migration had a mild anti-aliasing filter and a dense output grid of 12.5 m x 12.5 m. Even with traces from both Survey 1 and 2, the fold coverage of the migration input was still too sparse (Figure 1). Migration swings were not canceled out well in the Kirchhoff image, especially in the directions orthogonal to each survey's acquisition direction (Figure 2).

Limitation of pre-migration interpolation

One way to improve migration swing cancellation is to interpolate more traces to fill in the vacant bins. We performed pre-migration 3D interpolation after co-binning the dual-WAZ data. The migration of the data with pre-migration interpolation (Figure 3b) showed reduced swings and provided a better S/N. However, the resolution of the image was degraded. Shallow faults were smeared after pre-migration interpolation (Figure 3b) compared to dual-WAZ Kirchhoff migration without interpolation (Figure 3a). The large azimuth-offset differences between neighboring traces in the dual-WAZ data set posed a challenge to the interpolation, resulting in sub-optimal input for Kirchhoff migration.

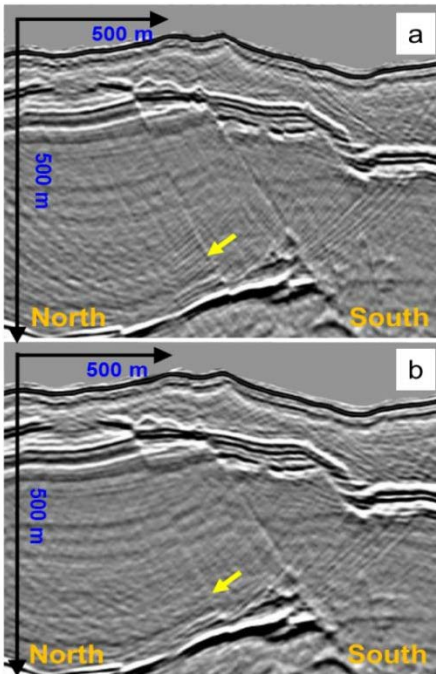

Figure 3: The dual-WAZ Kirchhoff image (a) without interpolation and (b) with pre-migration interpolation. The image with pre-migration interpolation has fewer swings; however, the faults are smeared by the interpolation, as indicated by the yellow arrows.

Preconditioned LS Kirchhoff migration for dual-WAZ

To fully retain the benefits of the dual-WAZ data set, we used preconditioned LS Kirchhoff migration to migrate the

10.1190/segam2018-2995491.1

two surveys with their original traces without pre-migration interpolation. The preconditioned LS Kirchhoff migration was able to handle the incomplete data and overcome migration artifacts, providing us with an elegant way to merge the dual-WAZ data.

LS migration inverts a reflectivity model m to fit the field data d_0 (Tarantola, 1987; Schuster, 1993; Nemeth et al., 1999). Its cost function $f(m)$ can be written as

$$f(m) = \frac{1}{2}\|d_0 - Lm\|^2, \quad (1)$$

where L is the demigration operator. The least-squares solution to this problem is

$$m = (L^T L)^{-1} L^T d_0, \quad (2)$$

where L^T is the migration operator and $L^T L$ is the Hessian matrix. Wang et al. (2016) proposed a single-iteration LS PSDM approach based on an approximation of the inverse Hessian matrix with curvelet-domain Hessian filters (CHF):

$$m_1 = C(m_0), \quad (3)$$

where m_0 is the initial migrated image, m_1 is the image after the first iteration of LS migration, and C is the CHF operator. Wang et al. (2017) extended the CHF approach to iterative LS migration. The approximate inverse Hessian is applied to every iteration of the gradient prior to obtaining the reflectivity for the next iteration. This approach provides the solutions to LS migration after the first iteration:

$$m_{i+1} = m_i + C[L^T(d_0 - Lm_i)]. \quad (4)$$

In addition to mitigating migration artifacts and compensating for illumination effects, the CHF operator also speeds up the LS migration convergence rate.

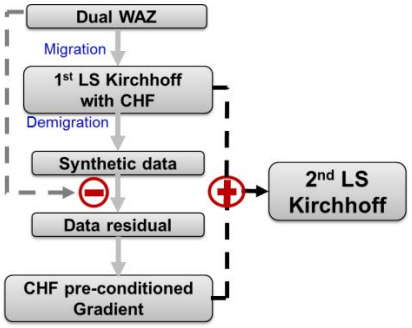

Figure 4: A flow chart for two iterations of CHF pre-conditioned dual-WAZ LS Kirchhoff migration.

In our LS Kirchhoff migration flow, we first binned the dual-WAZ data together and performed dual-WAZ Kirchhoff migration to get the initial image m_0 without pre-migration interpolation. We then demigrated m_0, followed by a re-migration to compute CHF operators by comparing m_0 against the re-migration. The CHF operators were applied to m_0 to obtain the first LS Kirchhoff image m_1. Further iterations involved demigrating the previous iteration image m_i and computing the residuals with respect to the recorded data. These residuals were then migrated and preconditioned using the CHF operators to obtain the new gradient g_i and the new output $m_{i+1} = m_i + g_i$. This iterative flow can be carried out with further iterations until the residual has no apparent signal energy. A flow chart for two iterations of dual-WAZ LS Kirchhoff

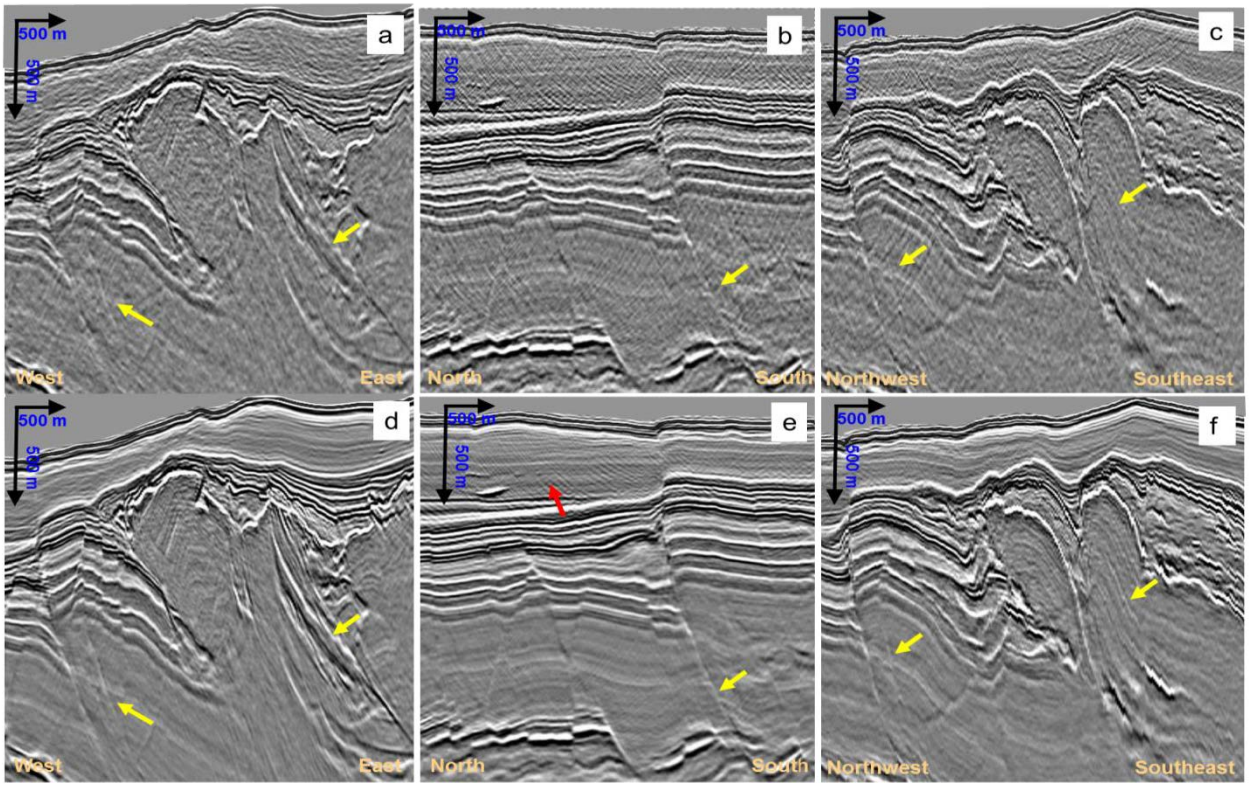

Figure 5: The dual-WAZ LS Kirchhoff images (d, e, and f) are significantly cleaner than dual-WAZ raw Kirchhoff (a, b, and c). The faults and other dipping overburden structures are better imaged by LS Kirchhoff as marked by yellow arrows. In the north-south direction, which is orthogonal to survey 1, there are residual swings observed after LS Kirchhoff (the red arrow in e).

migration is shown in Figure 4. After two iterations of dual-WAZ LS Kirchhoff migration, the residuals were significantly reduced and we found the results satisfactory.

The dual-WAZ LS migration was able to attenuate migration artifacts effectively and, at the same time, retained all the recorded details. The S/N in the dual-WAZ LS Kirchhoff migration result (Figures 5d-f) is better than in the raw dual-WAZ Kirchhoff migration (Figures 5a-c). Faults and complex shallow features (yellow arrows) are better imaged in the dual-WAZ LS Kirchhoff migration as well. Along the north-south orientation, the trace sampling is not optimal, and we observe some residual swings (red arrow) in Figure 5e. Additionally, the spectrum of dual-WAZ LS Kirchhoff migration is broader than dual-WAZ Kirchhoff migration (Figure 6).

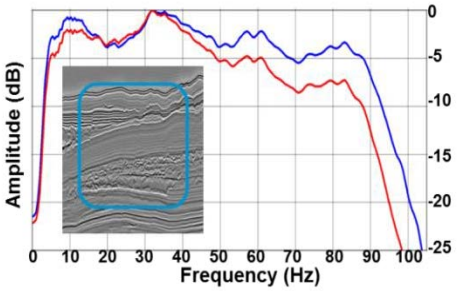

Figure 6: Dual-WAZ LS Kirchhoff migration (blue curve) has a wider spectrum than dual-WAZ Kirchhoff migration (red curve). The spectra were measured inside the light blue box.

From the data domain QC, the demigrated data after two iterations of dual-WAZ LS Kirchhoff migration matched well with the real data (Figure 7d vs Figure 7a). The data domain residuals were greatly reduced after dual-WAZ LS Kirchhoff migration (Figure 7e) compared to the residual after raw dual-WAZ Kirchhoff migration (Figure 7c), which was the starting point of this flow. Small data domain residual means the recorded dual-WAZ time data was well explained by the depth domain image.

Conclusion and discussion

Trace sparsity and azimuthal differences pose great challenges to merging WAZ surveys for shallow imaging. Pre-migration interpolation is often not optimal when we have multiple surveys with different azimuths.

Our results show that preconditioned LS Kirchhoff migration is an effective way to merge dual-WAZ together. It takes full advantage of the information recorded in the dual-WAZ data while also mitigating migration artifacts. With this iterative LS migration flow, we can overcome some drawbacks from poor trace density typical of WAZ surveys. We have successfully migrated dual-WAZ data with two iterations of LS Kirchhoff on a fine grid (12.5 m x 12.5 m), providing high-resolution shallow images.

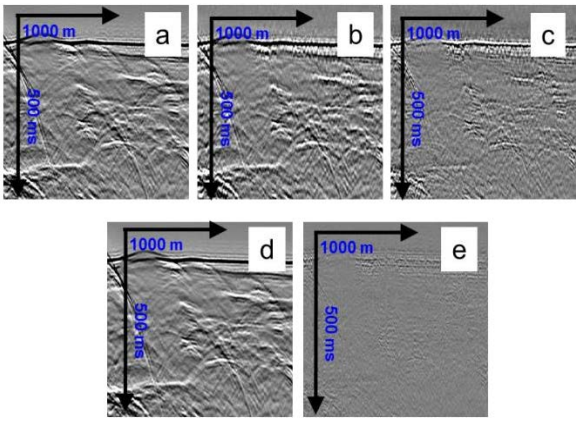

Figure 7: In the data domain, at offset 900 m, (d) demigrated data after two iterations of dual-WAZ LS Kirchhoff migration are closer to (a) input data than (b) demigrated data after raw dual-WAZ Kirchhoff migration. (e) The data domain residual (input – demigration output) after two iterations of LS Kirchhoff migration is significantly smaller than (c) the residual after raw Kirchhoff migration.

This flow handles survey merging at the migration stage with LS migration. It requires good pre-processing for each survey and carefully designed survey matching between the dual-WAZ surveys before migration. This process can be extended to merge any number of different surveys together.

A well-known but often overlooked aspect of LS migration is the velocity parameters used for the migration. For the best LS image with the least residuals, a good velocity that is derived using all the data sets involved in the migration is required. Lack of a good velocity may result in destructive interference of events from different surveys and often does not guarantee convergence.

LS Kirchhoff migration for a single WAZ survey can help produce better shallow images compared to conventional Kirchhoff migration, to some extent. However, LS Kirchhoff migration cannot be used to substitute for dense acquisitions. We still observed residual swings in the dual-WAZ LS Kirchhoff migration image and could observe more residual swings in the case of single WAZ.

Acknowledgments

We thank CGG for permission to publish the results. We thank Victor Lopez for preparing the data. We also thank our internal reviewers, Sabaresan Mothi, Tony Huang, and Shannon Basile for their valuable insights and comments.

10.1190/segam2018-2995491.1

REFERENCES

Nemeth, T., C. Wu, and G. T. Schuster, 1999, Least-squares migration of incomplete reflection data: Geophysics, **64**, 208–221, https://doi.org/10.1190/1.1444517.

Schuster, G. T., 1993, Least-squares cross-well migration: 63rd Annual International Meeting, SEG, Expanded Abstracts, 110–113, https://doi.org/10.1190/1.1822308.

Tarantola, A., 1987, Inverse problem theory: Methods for data fitting and model parameter estimation: Elsevier Science Publishing Company.

Wang, M., S. Huang, and P. Wang, 2017, Improved iterative least-squares migration using curvelet-domain Hessian filters: 87th Annual International Meeting, SEG, Expanded Abstracts, 4555–4560, https://doi.org/10.1190/segam2017-17783350.1.

Wang, P., A. Gomes, Z. Zhang, and M. Wang, 2016, Least-squares RTM: Reality and possibilities for subsalt imaging: 86th Annual International Meeting, SEG, Expanded Abstracts, 4204–4209, https://doi.org/10.1190/segam2016-13867926.1.

Wang, P., S. Ray, and K. Nimsaila, 2014, 3D joint deghosting and crossline interpolation for marine single-component streamer data: 84th Annual International Meeting, SEG, Expanded Abstracts, 3594–3598, https://doi.org/10.1190/segam2014-0882.1.